

Lewis-Base Stabilized *N*-Silver(I) Succinimide Complexes: Synthesis, Crystal Structures and Their Use as CVD-Precursors

Xian Tao,^[a] Ke-Cheng Shen,^[a] Yu-Long Wang,^[a] and Ying-Zhong Shen^{*[a]}

Keywords: Silver; Succinimide; X-ray diffraction; MOCVD; Vapor deposition

Abstract. Four Lewis-base stabilized *N*-silver(I) succinimide complexes of type $[L_n \cdot R_m \cdot \text{AgNC}_4\text{H}_4\text{O}_2]$ ($L = N,N,N',N'$ -tetramethylethylenediamine (TMEDA), $n = 1, m = 0$, **2a**; $L = \text{P}(\text{OEt})_3$, $n = 2, m = 0$, **2b**; $L = \text{PPh}_3$, $m = 0, n = 2$, **2c**; $L = \text{P}(\text{OMe})_3$, $R = \text{TMEDA}$, $n = 1, m = 1$, **2d**) were prepared by a “one-pot” synthesis methodology and characterized. The molecular structures of **2a** and **2c** have been determined by using X-ray single crystal analysis. Complex **2a** exists as

ion pair $\{\text{[Ag(TMEDA)}_2]^+[\text{Ag}(\text{NC}_4\text{H}_4\text{O}_2)]^-\}$ in the solid state and complex **2c** is a monomer with the three-coordinate silver atom. Complex **2b** was used as precursor in the deposition of silver for the first time by using MOCVD technique. The silver films obtained were characterized using scanning electron microscopy (SEM) and energy-dispersion X-ray analysis (EDX). SEM and EDX studies show that the dense and homogeneous silver films could be obtained.

Introduction

In recent years, owing to the highest electrical conductivity and the lowest contact resistance among all metals,^[1–5] silver has been widely used in many fields include: optical devices,^[6] components in high temperature superconductor materials,^[7] magnetic,^[8] bactericidal coatings^[9] and interconnect material in microelectronics.^[10] Various methods have been used for the growth of silver thin films, such as sputtering,^[11] thermal evaporation,^[12] electron-beam evaporation,^[13] and chemical vapor deposition (CVD).^[14] Metal Organic Chemical Vapor Deposition (MOCVD) is a very effective technique for the growth of high quality metal films due to the high deposition rates with good step coverage^[15–18] and higher aspect ratio in the multilevel metallization structure.^[19]

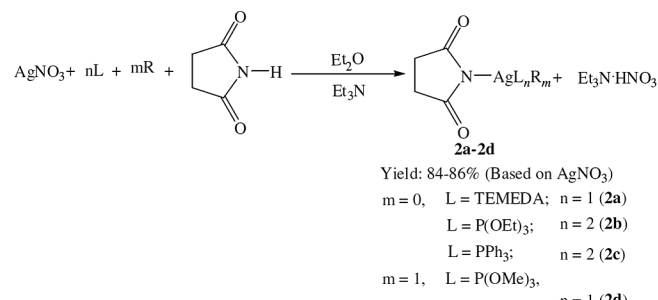
The key to achieve success for MOCVD, however, is the selection of suitable precursors. As the precursors for MOCVD, the complexes should have good volatility, thermal stability, high purity and a suitable thermal decomposition mechanism.^[20,21] Before, the research of silver precursors has focused mainly on silver(I) β -diketonates or structurally related complexes,^[22–26] silver(I) carboxylates,^[27–31] with various Lewis-base ancillary ligands. However, the precursors are not sufficiently available and the decomposition mechanism(s) are unclear. The development of new silver precursors is indispensable. In this paper, we describe different synthesis methodologies and properties of four Lewis-base stabilized *N*-silver(I) succinimide complexes which were used as precursor for the growth of silver by using MOCVD techniques. The single

crystal structures of **2a** and **2c** were determined and discussed as well.

Results and Discussion

Synthesis

The Lewis-base stabilized *N*-silver(I) succinimide complexes of type $[L_n \cdot R_m \cdot \text{AgNC}_4\text{H}_4\text{O}_2]$ ($L = N,N,N',N'$ -tetramethylethylenediamine (TMEDA), $n = 1, m = 0$, **2a**; $L = \text{P}(\text{OEt})_3$, $n = 2, m = 0$, **2b**; $L = \text{PPh}_3$, $m = 0, n = 2$, **2c**; $L = \text{P}(\text{OMe})_3$, $R = \text{TMEDA}$, $m = 1, n = 1$, **2d**) were prepared by using the consecutive reaction of $[\text{AgNO}_3]$, auxiliary donor ligands, succinimide and Et_3N by a “one-pot” synthesis methodology (Experimental Section) (Scheme 1). The complexes were isolated in high yield as colorless solids (**2a**, **2c**) or colorless liquids (**2b**, **2d**). Complexes **2a**–**2c** are stable under inert atmosphere for months at room temperature, but complex **2d** is sensitive to temperature and must be stored at 0°C . On exposure to air they all decompose within minutes (**2a**, **2d**) or hours (**2b**, **2c**) to form brown products. All products obtained gave satisfactory elemental analysis results and were characterized by FT-IR, ^1H NMR and ^{13}C {H} NMR spectroscopy, respectively.

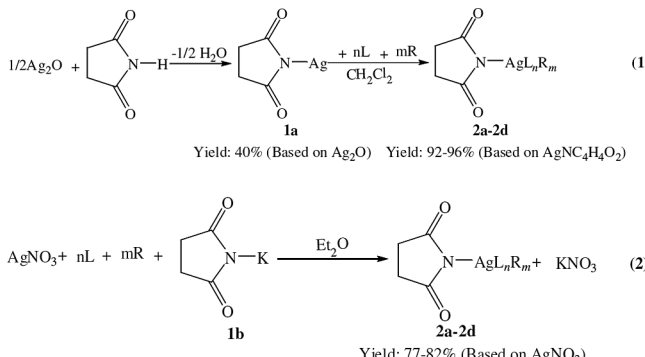


Scheme 1. Synthesis of Complexes **2a**–**2d**.

* Prof. Dr. Y.-Z. Shen
Fax: +86-25-52112626
E-Mail: yz_shen@nuaa.edu.cn

[a] Applied Chemistry Department
School of Material Science & Engineering
Nanjing University of Aeronautics & Astronautics
Nanjing 210016, P. R. China

The complexes also could be prepared by using auxiliary donor ligands reacting with *N*-silver(I) succinimide in dichloromethane in stoichiometry at 0 °C in relation to the reported synthesis procedures (Equation (1)),^[32] or by reaction of [AgNO₃] with auxiliary donor ligands and [KNC₄H₄O₂] in diethyl ether at 0 °C (Equation (2)). The disadvantage of the synthesis procedures described in Equation (1) for **2a–2d** is the low yield of *N*-silver(I) succinimide (Yield: 40 % based on Ag₂O) given by using succinimide reacting with an excess of Ag₂O in boiling water.^[32] Another adversarial aspect is the use of *N*-silver(I) succinimide with no coordinated ligand, since it shows the tendency to decompose on prolonged storage. The disadvantage of the synthesis procedures described in Equation (2) for **2a–2d** is the purification because some products may contain traces of chloride which is detrimental to their use as CVD precursors in microtechnology. Therefore, we developed a “one-pot” synthesis methodology to prepare Lewis-base stabilized *N*-silver(I) succinimide complexes. These preparative studies show that an economical and straightforward synthesis route was presented.



The spectra of metal succinimide complexes were investigated by *Woldbaek, Klaeboe, and Christensen*.^[33] In the IR spectra, the broad N–H stretching band ($\sim 3170 \text{ cm}^{-1}$) of succinimide disappeared in the complexes, as well as the sharp out-of-plane N–H bending band ($\sim 820 \text{ cm}^{-1}$).^[33] Due to the delocalization of the anionic charge to the ring and carbonyl groups, thus decreasing the C=O bond order.^[32] In the *N*-silver(I) succinimide complexes, the in-phase and out-of-phase stretching vibrations of the C=O groups are observed between 1700–1710 cm^{-1} and 1590–1619 cm^{-1} , respectively. In complexes **2b** and **2d**, the P–O stretching vibration in organophosphine ligands shifted to higher frequencies in the complexes provides the good evidence that the occurrence of the organophosphine ligands coordinating to silver ion.

The NMR spectra (¹H and ¹³C{H}) were recorded for all four complexes at room temperature. In ¹H NMR spectra, the integration area ratios are in agreement with the stoichiometries of the complexes. The chemical shifts of –CH₂– protons in C₄H₄NO₂[–] appeared at $\delta = 2.50$ –2.63 ppm, which agrees well with a previous report.^[32] In complex **2d**, the chemical shifts of alkyl protons of TMEDA [$\delta = 2.31$ (s, 12 H, (CH₃)₂N), $\delta = 2.43$ (s, 4 H, NCH₂) and P(OMe)₃ [$\delta = 3.71$ (d, 9 H, CH₃O, $J_{PH} = 13.1 \text{ Hz}$)] shifted to downfield compared to free ancillary ligands. In the ¹³C NMR spectra, the chemical

shifts of all carbonyl are found in the range of 191–192 ppm, which are similar to those of other metal succinimide complexes.^[32] In complex **2d**, the alkyl carbon resonances of TMEDA and trimethylphosphite are in the range of 47–58 ppm. However, the carbon resonances of ancillary ligands in **2a–2d** are easily distinguished from the resonance of –CH₂– on C₄H₄NO₂[–] (31.8–32.5 ppm).

Structural Analysis

The molecular structures of **2a** and **2c** are depicted in Figure 1 and Figure 2, and selected bond lengths /Å and bond angles /° are given in Table 1 and Table 2, respectively.

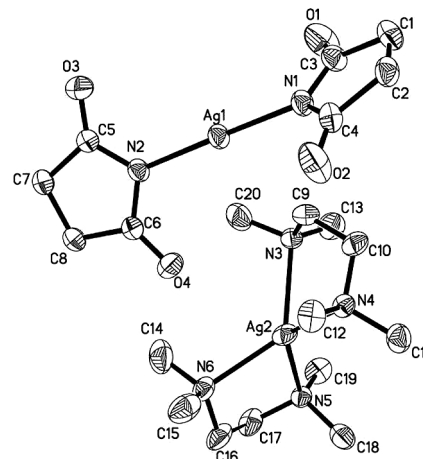


Figure 1. Molecular structure and atom numbering scheme for **2a**. The hydrogen atoms are omitted for clarity.

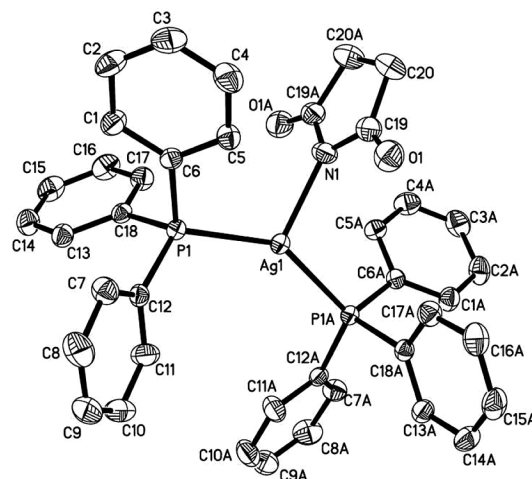


Figure 2. Molecular structure and atom numbering scheme for **2c**. The hydrogen atoms are omitted for clarity.

Complex **2a** crystallizes in a monoclinic in the space group $P2_1/c$. Ion pair $\{[\text{Ag}(\text{TMEDA})_2]^+[\text{Ag}(\text{NC}_4\text{H}_4\text{O}_2)_2]^- \}$ exhibits no contact distances between anion and cation in the solid state (Figure 1). In the cation, the silver(I) atom [Ag(2)] is presented with four nitrogen atoms of two TMEDA ligands occupying

Table 1. Selected bond lengths /Å and angles /° for **2a**.

Bond lengths /Å			
Ag(1)–N(2)	2.083(2)	Ag(2)–N(3)	2.389(2)
Ag(1)–N(1)	2.084(2)	C(6)–O(4)	1.218(3)
Ag(2)–N(4)	2.369(2)	C(3)–O(1)	1.215(4)
Ag(2)–N(6)	2.369(2)	C(5)–O(3)	1.214(3)
Ag(2)–N(5)	2.388(2)	C(4)–O(2)	1.216(4)
Bond angles /°			
N(2)–Ag(1)–N(1)	177.9(9)	C(11)–N(4)–Ag(2)	112.3(18)
N(4)–Ag(2)–N(6)	128.9(8)	C(12)–N(4)–Ag(2)	107.4(17)
N(4)–Ag(2)–N(5)	130.5(8)	C(10)–N(4)–Ag(2)	106.6(15)
N(6)–Ag(2)–N(5)	77.6(8)	C(5)–N(2)–Ag(1)	128.6(18)
N(4)–Ag(2)–N(3)	77.7(8)	C(6)–N(2)–Ag(1)	121.1(17)
N(6)–Ag(2)–N(3)	127.4(8)	C(4)–N(1)–Ag(1)	124.7(18)
N(5)–Ag(2)–N(3)	122.3(8)	C(3)–N(1)–Ag(1)	124.5(19)

Table 2. Selected bond lengths /Å and angles /° for **2c**.

Bond lengths /Å			
Ag(1)–N(1)	2.220(3)	C(19)–C(20)	1.506(5)
Ag(1)–P(1)	2.443(8)	C(20)–C(20) ^a	1.503(7)
O(1)–C(19)	1.217(4)	N(1)–C(19)	1.364(4)
Bond angles /°			
N(1)–Ag(1)–P(1)	107.3(18)	O(1)–C(19)–N(1)	124.0(3)
P(1) ^a –Ag(1)–P(1)	145.4(4)	O(1)–C(19)–C(20)	125.5(3)
C(19) ^a –N(1)–C(19)	110.6(4)	N(1)–C(19)–C(20)	110.4(3)
C(19)–N(1)–Ag(1)	124.7(19)	C(20) ^a –C(20)–C(19)	104.1(2)
Symmetry operation: a = -x-1; y; -z - 3/2			

four coordination sites, forming a distorted tetrahedral arrangement. The two perpendicular planes of the $[\text{Ag}(\text{TMEDA})_2]^+$, defined by [N(3), Ag(2), N(4)] and [N(5), Ag(2), N(6)], respectively, are almost vertical as indicated by the dihedral angle (86.4°), which is close to the ideal value (90°). The atoms [N(1), Ag(1), N(2)] of the $[\text{Ag}(\text{NC}_4\text{H}_4\text{O}_2)_2]^-$ cluster anion core, approximately form a line with an angle of $177.9(9)^\circ$. The dihedral angle of two roughly planar succinimide rings is 115.9° . The average distances of Ag–N (2.379 \AA) is longer than that of $[\text{Ag}(\text{hfac})(\text{TMEDA})]$ [$2.255(5) \text{ \AA}$].^[34] Three groups of the average angle of N–Ag(2)–N (129.7° , 77.6° , 124.8°) are close to that of $[\text{Ag}(\text{lb})_2\text{OTf}]$ (132.7° , 76.3° , 123.7°) ($\text{lb} = \text{C}_{16}\text{H}_{14}\text{N}_2\text{Br}_2$).^[35]

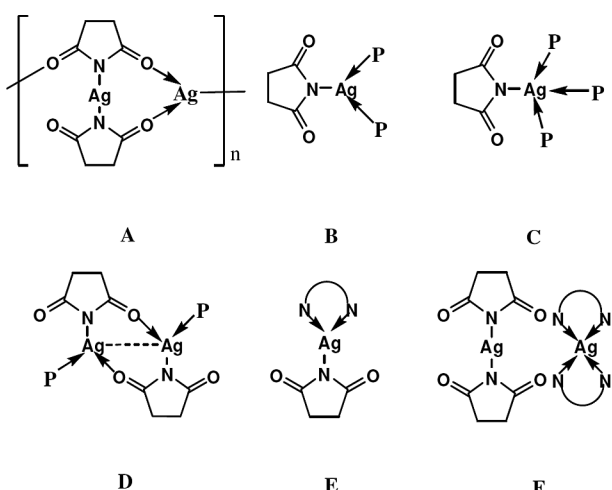
Complex **2c** has a crystallographic C_2 symmetry axis passing through the Ag(1)–N(1) vector. (Figure 2) It crystallizes in a monoclinic in the space group $C2/c$, and a three-coordinate silver(I) ion is presented with two phosphorus atoms from PPh_3 ligands occupying two coordination sites (PP) and the nitrogen atom from succinimide occupying the third site. Four atoms [P(1), N(1), P(1)^a, Ag(1)] are in the same plane, forming an isosceles triangle geometry around silver. The C(55)–C(56)–C(57)–C(58) plane and P(1)–N(1)–P(1)^a–Ag(1) plane are roughly perpendicular to each other and the dihedral angle is 80.3° . The P–Ag–P angle [$145.4(5)^\circ$] is much larger than that of $[(\text{Ph}_3\text{P})_2\text{AgPI}]$ [$116.6(3)^\circ$] (PI = $\text{C}_8\text{H}_4\text{NO}_2$), but the N–Ag–P angle [$107.3(18)^\circ$] is much smaller than that of $[(\text{Ph}_3\text{P})_2\text{AgPI}]$ [$121.7(2)^\circ$] (PI = $\text{C}_8\text{H}_4\text{NO}_2$).^[33] In this mono-

meric succinimide complex, the three-coordinate nature of the silver seems to be quite a satisfactory bonding environment.

The Ag–P bond length in complex **2c** [$2.443(8) \text{ \AA}$] is almost the same to the sum of covalent radii of the phosphorus and silver atoms (2.44 \AA).^[36] The N–Ag distance in **2a** and **2c** is $2.084(2) \text{ \AA}$, $2.083(2) \text{ \AA}$ and $2.220(3) \text{ \AA}$, respectively, which are all shorter than that of $[(\text{Ph}_3\text{P})_3\text{AgNC}_4\text{H}_4\text{O}_2]$ [$2.313(4) \text{ \AA}$].^[32] The average distances of C–O (1.216 \AA), of which the oxygen atoms do not chelate to the silver, is obviously shorter than those of $[(\text{MeO})_3\text{P}\cdot\text{AgNC}_4\text{H}_4\text{O}_2]_2$ [(C(1)–O(1): $1.243(4) \text{ \AA}$; C(5)–O(3): $1.233(5) \text{ \AA}$].^[37] Comparison to complex $[(\text{MeO})_3\text{P}\cdot\text{AgNC}_4\text{H}_4\text{O}_2]_2$,^[37] which has an Ag–O bond, complexes **2a** and **2c** have the symmetrically centered Ag–N with equidistant separations between the silver and oxygen.

In general, silver(I) salts of structural type $[\text{Ag}X]$ (X = organic or inorganic group) are highly aggregated.^[38–40] These building blocks can be broken-down to lower aggregated species by the addition of Lewis-bases.

Silver(I) succinimide $[\text{AgNC}_4\text{H}_4\text{O}_2]_n$ with no auxiliary donor ligands have been shown to form oligomers with a variety of structural motifs,^[40,41] but including mainly dimers with crude flat eight-membered rings **A**, the arrangement of which is clearly codetermined by forming of Ag–O bonds (Scheme 2). With donor ligands P (P = PPh_3 or $\text{P}(\text{OMe})_3$), the ring systems of 1:2 complexes $[(\text{P})_2\text{AgNC}_4\text{H}_4\text{O}_2]_n$ and 1:3 complexes $[(\text{P})_3\text{AgNC}_4\text{H}_4\text{O}_2]_n$, cannot remain intact except 1:1 complexes $[(\text{P})\text{AgNC}_4\text{H}_4\text{O}_2]_n$.^[32,37] The coordination number (CN) of the metal atoms increase to 3 or 4 in these complexes, which lose the Ag–Ag contacts as in **B** and **C**,^[32] or preserve metalophilic bonding as in **D**.^[37] However, with donor ligands N N (N N = bipy or N,N,N',N' -tetramethylethylenediamine), the ring systems of 1:1 complexes $[(\text{N N})\text{AgNC}_4\text{H}_4\text{O}_2]_n$ are destroyed with the different coordination number (CN) of the metal atoms from 2 to 4 as **E**^[42] and **F**. The special structure as **F** exhibits no contact distances between anion and cation with the two kinds of silver atoms which coordination number

**Scheme 2.** Schematic representation of structural type **A–F** molecules.^[30,38,44]

(CN) are 2 and 4, respectively. It should be noted that the structural chemistry of the silver succinimide is entirely different. Only large ligands and the numbers of auxiliary donor ligands may prevent the close approach necessary for bonding Ag···Ag contacts and the forming of oligomers.

Thermal Analysis

Thermogravimetry (TG) and Differential Scanning Calorimetry (DSC) studies are required to optimize the temperature at which the respective silver precursor should be maintained during the CVD experiments. For an example, the TG and DSC curves of complex **2c** are shown in Figure 3. It can be seen from the DSC curve of **2c** that one apparent endothermic process with the peak temperatures at 208 °C, which could be attributed to the melting process of complex. There are two continuous exothermic/endothermic processes from 210 °C to 261 °C with the peak temperatures at 237 °C and 255 °C. Seen from the TG curve of **2c**, it is very difficult to distinguish from one step to another and know the sequence of decomposition of PPh₃ and succinimide. The final percentage of the residue is 16.06 %, which is little higher than the theoretical value of silver (14.77 %). The thermal measurement is in good agreement with the structural analysis.

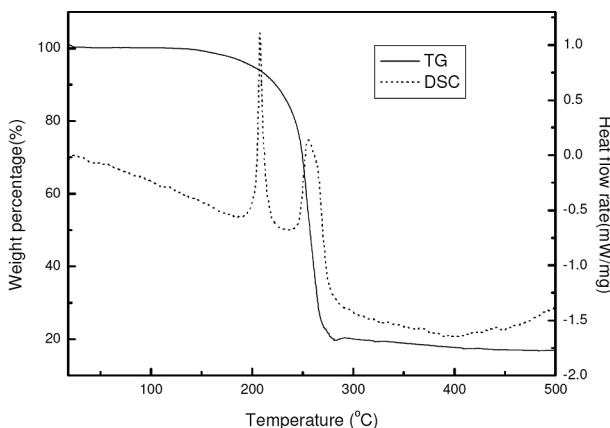


Figure 3. TG and DSC curves of **2c** (heating rate 10 °C · min⁻¹, argon atmosphere).

MOCVD Depositions

On the basis of the thermal properties obtained from the TG and DSC studies and Ref.,^[32] we find these complexes may be promising precursors for the growth of silver films. The complex **2b** has been successfully applied to deposit silver on silicon substrates by MOCVD. In a typical CVD experiment silver was deposited onto silicon substrate at 350 °C. The evaporation temperature was maintained at 80 °C with a nitrogen flow rate at 20 sccm. The run time was 1.5 h and the total pressure was kept at 7.0 × 10⁻⁴ bar. No reducing reagent such as H₂ was used in the deposition process. The average film thickness was about 0.9 μm, giving a growth rate of 0.6 μm · h⁻¹. The layer deposited is silver colored. The surface

morphology and composition of the silver film were characterized by scanning electron microscopy (SEM) and energy-dispersive X-ray analysis (EDX). SEM (Figure 4) studies show that the dense and homogeneous silver layer was formed. The film is composed of many well isolated, granular genuine pearls spreading all over the substrate. The sizes of silver grains are in the range of 40–60 nm.

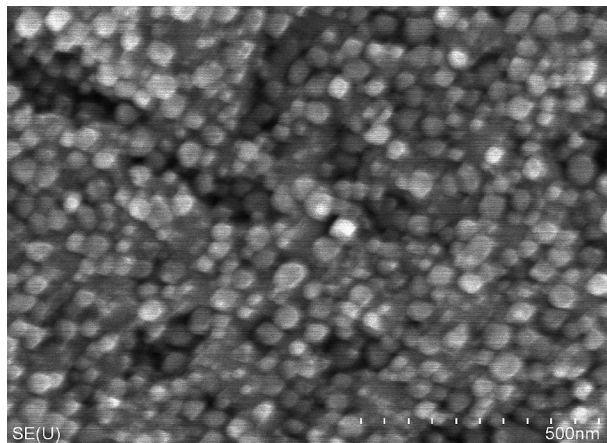


Figure 4. SEM spectrum of the silver film deposited from **2b** ($T_s = 350$ °C, $p_{\text{total}} = 7.0 \times 10^{-4}$ bar; carrier gas N₂; flow rate = 20 sccm).

The EDX spectrum (Figure 5) of the deposited film shows silver as the main component. Next to silver, silicon as substrate component was detected which is due to the discontinuous silver particles and the relatively high penetration depth of the electron beam during the EDX analysis. The other light elements, such as carbon, oxygen, phosphorus, which might be present as impurities or due to a surface oxidation of silver, are below the detection limit.

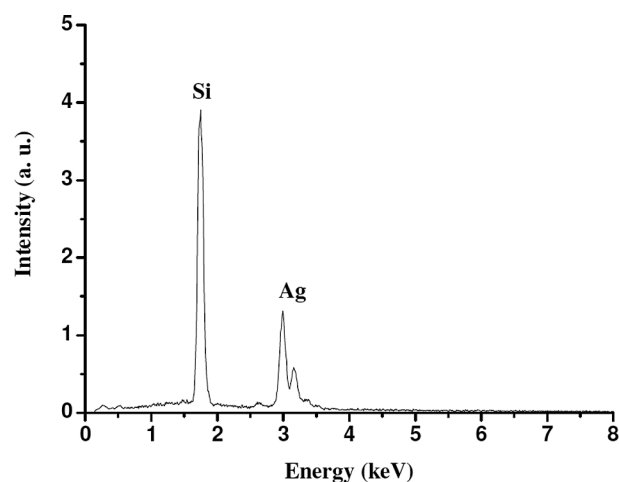


Figure 5. EDX spectrum of the silver film deposited from **2b** ($T_s = 350$ °C, $p_{\text{total}} = 7.0 \times 10^{-4}$ bar; carrier gas N₂; flow rate = 20 sccm).

The result of this deposition experiment shows that complex **2b** is a promising candidate for further MOCVD process of silver nanocluster or silver films.

Conclusions

Four Lewis-base stabilized *N*-silver(I) succinimide complexes has been synthesized by a “one-pot” synthesis methodology which is economical and straightforward. Complex **2a** exists as ion pair $\{[\text{Ag}(\text{TMEDA})_2]^+[\text{Ag}(\text{NC}_4\text{H}_4\text{O}_2)_2]^- \}$ in the solid state and complex **2c** is a monomer with the three-coordinate silver atom. In deposition experiments complex **2b** was used as MOCVD precursor to grow silver layers on silicon substrates at 350 °C deposition temperature, carrier gas flow 20 sccm, and a total pressure of 7.0×10^{-4} bar, respectively. The film is composed of many well isolated, granular genuine pearls spreading all over the substrate. The EDX results showed that the obtained layer composed of pure silver within the detection limit of EDX.

Experimental Section

Materials and Methods

All operations were carried out under an atmosphere of purified nitrogen with standard Schlenk techniques. The solvent diethyl ether was purified by distillation from sodium/benzophenone under N₂ before use. ¹H NMR were recorded with a Bruker DRX500 NMR spectrometer operating at 500.13 MHz in the Fourier transform mode; ¹³C{H} NMR spectra were recorded at 125.76 MHz. Chemical shifts are reported in δ units (parts per million) downfield from tetramethylsilane ($\delta = 0.0$) with the solvent as the reference signal (¹H NMR, CDCl₃ $\delta = 7.26$; ¹³C{H} NMR, CDCl₃ $\delta = 77.55$). Infrared spectra were collected on Bruker Vector 22 instrument as KBr pellets at room temperature. Thermogravimetric (TG) and Differential Scanning Calorimetric (DSC) studies were carried out with the NETZSCH STA 449 C with a constant heating rate of 10 °C·min⁻¹ under Argon (30 cm³·min⁻¹). Elemental analysis was performed with a Perkin–Elmer 240 C elemental analyzer. Melting points were measured in sealed capillaries and were uncorrected. The MOCVD experiments were carried out vertical quartz tube hot-wall MOCVD reactor with 60 mm in diameter. Heating was achieved by a resistively heated tube oven (AICHUANG Company). The temperature was set by a temperature control FP 93 (SHIMADEN Company) and was calibrated with a thermocouple type SR 3 (SHIMADEN Company) digital thermometer. The precursor container was heated with a heating band for evaporation of the precursor. The precursor vapor was transported to the reactor tube by N₂ carrier gas. The carrier gas flow was regulated using a D07–7B (SEVEN-STAR Company) mass flow controller which was connected to the apparatus by a section of flexible stainless steel tubing. The pressure control system consists of a cooling trap and a FT-110 (KYKY Company) molecular pump unit. The trap prevents the reactor effluents from entering the vacuum pump. SEM images and EDX analysis were carried out with Hitachi Model S-4800 with scanning electron microscope and energy dispersive X-ray detector.

Syntheses

$\{[\text{Ag}(\text{TMEDA})_2]^+[\text{Ag}(\text{NC}_4\text{H}_4\text{O}_2)_2]^- \}$ (**2a**): To a solution of *N,N,N',N'*-tetramethylethylenediamine (0.4648 g, 4.00 mmol), succinimide (0.3964 g, 4.00 mmol) and AgNO₃ (0.6795 g, 4.00 mmol) in dry diethyl ether (30 mL), triethylamine (0.4048 g, 4.00 mmol) was added. The clear solution was obtained by filtration through a pad of celite after stirring the reaction mixture for 6 h at 0 °C. A colorless solid product was obtained after removing all volatiles in oil-pump vacuo.

Yield: 1.09 g (85 % based on AgNO₃). Mp.: 165 °C dec. C₂₀H₄₀O₄Ag₂N₆: C, 37.28; H, 6.26. Found: C, 37.16; H, 6.02. ¹H NMR (CDCl₃): $\delta = 2.51$ (s, 12 H, CH₃/(CH₃)₂N–H), $\delta = 2.52$ (s, 4 H, NCH₂–H), 2.63 (s, 4 H, CH₂–). ¹³C{H} NMR (CDCl₃): $\delta = 32.2$ (CH₂), $\delta = 48.1$ (CH₃), $\delta = 58.0$ (CH₂/NCH₂–), $\delta = 191.6$ (C=O). IR (KBr) data: 3432 (m), 2928 (w), 1701 (m), 1619 (s), 1439 (m), 1359 (s), 1296 (s), 1249 (s), 827 (w), 669 (m), 570 (w), 451 (w) cm⁻¹.

$\{[(\text{EtO})_3\text{P}]_2\cdot\text{AgNC}_4\text{H}_4\text{O}_2 \}$ (**2b**): Complex **2b** was obtained by following the above procedure, only using triethylamine (0.5059 g, 5.00 mmol), triethylphosphite (1.6620 g, 10.00 mmol), succinimide (0.4955 g, 5.00 mmol) and AgNO₃ (0.8494 g, 5.00 mmol) instead. After appropriate work-up, complex **2b** was obtained as a colorless liquid. Yield: 2.26 g (84 % based on AgNO₃). C₁₆H₃₄O₄AgNP₂: C, 35.70; H, 6.37. Found: C, 35.57; H, 6.38. ¹H NMR (CDCl₃): $\delta = 1.2$ (t, 18 H, CH₃/CH₃CH₂–, $J_{HH} = 7.0$ Hz), $\delta = 2.5$ (s, 4 H, CH₂–H), 3.9 (m, 12 H, CH₂/CH₃CH₂–). ¹³C{H} NMR (CDCl₃): $\delta = 31.8$ (CH₂), $\delta = 191.0$ (C), 16.1 ($J_{PC} = 6.1$ Hz, CH₃/CH₃CH₂–), 60.0 ($J_{PC} = 5.7$ Hz, CH₂/CH₃CH₂–). IR (KBr) data: 3440 (m), 2979 (s), 2934 (m), 2901 (m), 2358 (w), 1715 (m), 1612 (s), 1477 (m), 1441 (m), 1391 (s), 1348 (s), 1287 (s), 1245 (s), 1162 (m), 1097 (m), 1022 (s), 937 (s), 771 (s), 669 (m), 536 (s), 442 (m) cm⁻¹.

$[(\text{Ph}_3\text{P})_2\cdot\text{AgNC}_4\text{H}_4\text{O}_2]$ (**2c**): Complex **2c** was synthesized following the synthesis of **2a**. In this respect, triethylamine (0.4048 g, 4.00 mmol) reacted with triphenylphosphine (2.0983 g, 8.00 mmol), succinimide (0.3964 g, 4.00 mmol) and AgNO₃ (0.6795 g, 4.00 mmol). After appropriate work-up, complex **2c** was isolated as a colorless solid. Yield: 2.46 g (84 % based on AgNO₃). Mp.: 196 °C dec. C₄₀H₃₄O₄AgNP₂: C, 65.77; H, 4.69. Found: C, 65.63; H, 4.63. ¹H NMR (CDCl₃): $\delta = 2.60$ (s, 4 H, CH₂–H), 7.30–7.44 (m, 30 H, Ph–H). ¹³C{H} NMR (CDCl₃): $\delta = 32.5$ (CH₂), $\delta = 192.4$ (C=O), 133.9 ($J_{PC} = 16.8$ Hz, C₆H₅), 132.6 ($J_{PC} = 24.1$ Hz, C₆H₅), 130.0 (C₆H₅), 128.7 ($J_{PC} = 9.5$ Hz, C₆H₅). IR (KBr) data: 3655 (m), 3049 (m), 2962 (m), 2361 (w), 1700 (m), 1603 (s), 1583 (m), 1478 (m), 1434 (s), 1345 (s), 1285 (s), 1247 (s), 1183 (w), 1095 (s), 1026 (m), 996 (m), 803 (m), 746 (s), 695 (s), 512 (s), 436 (m) cm⁻¹.

$\{[(\text{MeO})_3\text{P}] \cdot \text{AgNC}_4\text{H}_4\text{O}_2 \cdot (\text{TMEDA}) \}$ (**2d**): Complex **2d** was prepared by using a similar method for **2a**. In this respect, triethylamine (0.5059 g, 5.00 mmol) reacted with *N,N,N',N'*-tetramethylethylenediamine (0.5811 g, 5 mmol), trimethylphosphite (0.6205 g, 5 mmol), succinimide (0.4955 g, 5.00 mmol) and AgNO₃ (0.8494 g, 5.00 mmol). After appropriate work-up, complex **2d** was obtained as a colorless ropy liquid. Yield: 1.92 g (86 % based on AgNO₃). C₁₃H₂₉O₃AgN₃P: C, 34.99; H, 6.55. Found: C, 34.63; H, 6.36. ¹H NMR (CDCl₃): $\delta = 2.31$ (s, 12 H, CH₃/(CH₃)₂N–H), $\delta = 2.43$ (s, 4 H, NCH₂–H), $\delta = 2.62$ (s, 4 H, CH₂–H), 3.71 (d, 9 H, CH₃O–H, $J_{PH} = 13.1$ Hz). ¹³C{H} NMR (CDCl₃): $\delta = 32.2$ (CH₂), $\delta = 47.4$ (CH₃), $\delta = 51.3$ ($J_{PC} = 4.2$ Hz, CH₃/CH₂O–), $\delta = 58.0$ (CH₂/NCH₂–), $\delta = 191.7$ (C=O). IR (KBr) data: 3441 (m), 2929 (m), 2836 (m), 1700 (m), 1618 (s), 1439 (m), 1359 (s), 1391 (s), 1269 (s), 1248 (s), 1182 (w), 1013 (m), 790 (m), 761 (w), 669 (m), 570 (w), 452 (w) cm⁻¹.

Crystal Structure Determinations

Single crystals of **2a** and **2c** could be obtained by cooling a saturated diethyl ether solution to –20 °C. Suitable crystals for X-ray determination were placed in glue under N₂ due to its sensitivities to oxygen and moisture. X-ray structure measurement was performed with a Rigaku SCXmini CCD, detector equipped with graphite monochromatic Mo-K_α radiation ($\lambda = 0.71073$ Å), at room temperature. Date collection and processing (cell refinement, data reduction and empirical absorption

correction) were performed using the CRYSTALCLEAR program package.^[43] The structure was solved by direct methods using SHELXS-97^[44] and refined by full-matrix least-squares procedures on F^2 with SHELXL-97.^[45] All of the non-hydrogen atoms were refined with anisotropic displacement parameters. Crystallographic data and details on refinement are presented in Table 3. Crystallographic data for the structural analyses of **2a** and **2c** were deposited with the Cambridge Crystallographic Data Centre, CCDC-775778 for **2a** and CCDC-715554 for **2c**. Copies of this information may be obtained free of charge from The Director, CCDC, 12 Union Road, Cambridge CB2 1EZ, UK (Fax: +44-1223-336-033; or E-Mail: deposit@ccdc.cam.ac.uk or http://www.ccdc.cam.ac.uk).

Table 3. Crystallographic data and structure refinement details for **2a** and **2c**.

compound	2a	2c
Formula	$C_{20}H_{40}Ag_2N_6O_4$	$C_{40}H_{34}AgNO_2P_2$
Formula weight	644.32	730.49
Crystal Dimensions /mm	$0.2 \times 0.2 \times 0.2$	$0.3 \times 0.3 \times 0.2$
Crystal system	Monoclinic	Monoclinic
Space group	$P2_1/c$	$C2/c$
$a/\text{\AA}$	9.784(2)	8.856(18)
$b/\text{\AA}$	19.302(4)	16.624(3)
$c/\text{\AA}$	14.296(3)	23.139(5)
$\beta/^\circ$	90.63(3)	94.13(3)
$V/\text{\AA}^3$	2699.7(9)	3397.9(12)
Z value	4	4
$D_{\text{calc}}/\text{g}\cdot\text{cm}^{-3}$	1.585	1.428
Index ranges	$-12 \leq h \leq 10$, $-23 \leq k \leq 23$, $-13 \leq l \leq 17$	$-11 \leq h \leq 11$, $-21 \leq k \leq 21$, $-30 \leq l \leq 29$
$F(000)$	1312	1496
$\mu(\text{Mo}-K_{\alpha})/\text{mm}^{-1}$	1.49	0.723
$\lambda(\text{Mo}-K_{\alpha})/\text{\AA}$	0.71073	0.71073
Temperature /K	293(2)	293(2)
$2\theta_{\text{max}}/^\circ$	58	55
No. of refl. measured	5206	3909
Ind. refl. obs. [$I > 2\sigma(I)$]	4431	3199
No. of refined parameters	297	209
$R_1 [I > 2\sigma(\theta)]$	0.0310	0.041
$wR_2 [I > 2\sigma(\theta)]$	0.0664	0.082
Goodness-of-fit ^c	0.999	1.08
$\Delta\rho_{\text{max}}, \Delta\rho_{\text{min}}/\text{e}\cdot\text{\AA}^{-3}$	0.50, -0.94	0.56, -0.31

Acknowledgement

This work was supported by *Natural Science Foundation of Jiangsu Province* (BK2007199), *National Science and Technology of Major Project* (2009ZX02039101-02), *Funding of Jiangsu Innovation Program for Graduate Education* (CX10B-100Z) and *Outstanding Doctoral Dissertation in NUAA* (BCXJ10-11) were also acknowledged.

References

- [1] P. Piszczeck, E. Sylyk, M. Chaberski, C. Taeschner, A. Leonhardt, W. Bala, K. Bartkiewicz, *Chem. Vap. Deposition* **2005**, *11*, 53–59.
- [2] K. M. Chi, Y. H. Lu, *Chem. Vap. Deposition* **2001**, *7*, 117–120.
- [3] H. Schmidt, Y. Shen, M. Leschke, T. Haase, K. Kohse-Höinghaus, H. Lang, *J. Organomet. Chem.* **2003**, *669*, 25–31.
- [4] T. T. Kodas, M. J. Hampden-Smith, *The Chemistry of Metal CVD*, VCH, Weinheim, Germany, **1994**.
- [5] D. R. Smith, F. R. Fickett, *J. Res. Natl. Inst. Stand. Technol.* **1995**, *100*, 119–171.
- [6] M. W. Xu, S. J. Bao, X. G. Zhang, *Mater. Lett.* **2005**, *59*, 2194–2198.
- [7] A. Jakob, H. Schmidt, P. Djiele, Y. Z. Shen, H. Lang, *Microchim. Acta* **2007**, *156*, 77–81.
- [8] Y. F. Lu, M. Takai, S. Nagatomo, K. Kato, S. Namba, *Appl. Phys. A* **1992**, *54*, 51–56.
- [9] H. Liedberg, T. Lundeberg, *Urol. Res.* **1989**, *17*, 359–360.
- [10] W. Zhang, S. H. Brongersma, O. Richard, B. Brijs, R. Palmans, L. Froyen, K. Maex, *Microelectron. Eng.* **2004**, *76*, 146–152.
- [11] M. Hauder, W. Hansch, J. Gstootner, D. Schmitt-Landsiedel, *Appl. Phys. Lett.* **2001**, *78*, 838–840.
- [12] J. Uchil, K. Mohan Rao, M. Pattabi, *J. Phys. D* **1996**, *29*, 2992–2996.
- [13] A. C. Carter, W. Chang, S. B. Qadri, J. S. Horwitz, R. Leuchtner, D. B. Chrisey, *J. Mater. Res.* **1998**, *13*, 1418–1421.
- [14] A. Grodzicki, I. Lakomska, P. Piszczeck, I. Szymanska, E. Szlyk, *Coord. Chem. Rev.* **2005**, *249*, 2232–2258.
- [15] A. Jain, K. M. Chi, T. T. Kodas, M. J. Hampden-Smith, *J. Electrochem. Soc.* **1993**, *140*, 1434–1439.
- [16] N. Awaya, Y. Arita, *Proceedings of the 1991 Symposium on VLSI Technology*, Orso, Japan, **1991**, 37.
- [17] J. E. Parmeter, G. A. Petersen, P. M. Smith, C. A. Apblett, J. S. Reid, J. A. T. Norman, A. K. Hochberg, D. A. Roberts, T. R. Omstead, *J. Vac. Sci. Technol. B* **1995**, *13*, 130–136.
- [18] G. Braeckelmann, D. Manger, A. Burke, G. G. Peterson, A. E. Kaloyerous, C. Reidsema, T. R. Omstead, J. F. Loan, J. J. Sullivan, *J. Vac. Sci. Technol. B* **1996**, *14*, 1828–1836.
- [19] S. Kim, D. J. Choi, K. R. Yoon, K. H. Kim, S. K. Koh, *Thin Solid Films* **1997**, *311*, 218–224.
- [20] J. Rickerby, J. H. G. Steinke, *Chem. Rev.* **2002**, *102*, 1525–1550.
- [21] H. K. Shin, K. M. Chi, J. Farkas, M. J. Hampden-Smith, T. T. Kodas, E. N. Duesler, *Inorg. Chem.* **1992**, *31*, 424–431.
- [22] N. H. Dryden, J. J. Vittal, R. J. Puddephatt, *Chem. Mater.* **1993**, *5*, 765–766.
- [23] Z. Yuan, N. H. Dryden, J. J. Vittal, R. J. Puddephatt, *Chem. Mater.* **1995**, *7*, 1696–1702.
- [24] D. A. Edwards, R. M. Harker, M. F. Mahon, K. C. Molloy, *J. Mater. Chem.* **1999**, *9*, 1771–1780.
- [25] W. Lin, T. H. Warren, R. G. Nuzzo, G. S. Girolami, *J. Am. Chem. Soc.* **1993**, *115*, 11644–11645.
- [26] S. Serghini-Monim, Z. Yuan, K. Griffiths, P. R. Norton, R. J. Puddephatt, *J. Am. Chem. Soc.* **1995**, *117*, 4030–4036.
- [27] A. Grodzicki, I. Lakomska, P. Piszczeck, I. Szymanska, E. Szlyk, *Coord. Chem. Rev.* **2005**, *249*, 2232–2258.
- [28] S. Samoilenkova, M. Stefan, G. Wahl, S. Paramonov, N. Kuzmina, *Chem. Vap. Deposition* **2002**, *8*, 74–78.
- [29] T. Haase, K. Kohse-Höinghaus, B. Atakan, H. Schmidt, H. Lang, *Chem. Vap. Deposition* **2003**, *9*, 144–148.
- [30] E. Szlyk, P. Piszczeck, A. Grodzicki, M. Chaberski, A. Golinski, J. Szatkowski, T. Blaszczyk, *Chem. Vap. Deposition* **2001**, *7*, 111–116.
- [31] E. Szlyk, P. Piszczeck, I. Lakomska, A. Grodzicki, J. Szatkowski, T. Blaszczyk, *Chem. Vap. Deposition* **2000**, *6*, 105–108.
- [32] X. Tao, Y. Q. Li, H. H. Xu, N. Wang, F. L. Du, Y. Z. Shen, *Polyhedron* **2009**, *28*, 1191–1195.
- [33] D. R. Whitcomb, M. Rajeswaran, *J. Chem. Crystallogr.* **2006**, *36*, 587–598.
- [34] Z. Livio, B. Franco, N. Marco, R. Gilberto, Z. Pierrino, K. Sauvius, M. Alessio, *Chem. Vap. Deposition* **2004**, *10*, 207–213.
- [35] T. G. Richmond, E. P. Kelson, A. M. Arif, G. B. Carpenter, *J. Am. Chem. Soc.* **1988**, *110*, 2334–2335.
- [36] B. K. Teo, J. C. Calabrese, *Inorg. Chem.* **1976**, *15*, 2467–2474.
- [37] X. Tao, Y. L. Wang, K. C. Shen, Y. Z. Shen, *Inorg. Chem. Commun.* **2011**, *14*, 169–171.
- [38] P. Piszczeck, E. Sylyk, M. Chaberski, C. Taeschner, A. Leonhardt, W. Bala, K. Bartkiewicz, *Chem. Vap. Deposition* **2005**, *11*, 53–59.
- [39] K. M. Chi, Y. H. Lu, *Chem. Vap. Deposition* **2001**, *7*, 117–120.

- [40] H. Schmidt, Y. Shen, M. Leschke, T. Haase, K. Kohse-Höinghaus, H. Lang, *J. Organomet. Chem.* **2003**, *669*, 25–31.
- [41] D. R. Whitcomb, M. Rajeswaran, *Acta Crystallogr., Sect. E* **2007**, *63*, m2753.
- [42] D. R. Whitcomb, M. Rajeswaran, *Acta Crystallogr., Sect. E* **2007**, *63*, m1179–m1181.
- [43] Rigaku/MSC, *CRYSTALCLEAR*, Rigaku/MSC Inc., The Woodlands, Texas, USA, **2005**.
- [44] G. M. Sheldrick, *SHELXS-97*, Structure Solving Program, University of Gottingen, Germany, **1997**.
- [45] G. M. Sheldrick, *SHELXL-97*, Crystal Structure Refinement Program, University of Gottingen, Germany, **1997**.

Received: February 13, 2011

Published Online: May 23, 2011